PTEP

Prog. Theor. Exp. Phys. **2014**, 101D02 (7 pages)
DOI: 10.1093/ptep/ptu134

Letter

Proton radius of ^{14}Be from measurement of charge-changing cross sections

S. Terashima[1,*], I. Tanihata[1,2,*], R. Kanungo[3], A. Estradé[3,4], W. Horiuchi[5], F. Ameil[4], J. Atkinson[2], Y. Ayyad[6], D. Cortina-Gil[6], I. Dillmann[4], A. Evdokimov[4], F. Farinon[4], H. Geissel[4], G. Guastalla[4], R. Janik[7], M. Kimura[5], R. Knoebel[4], J. Kurcewicz[4], Yu. A. Litvinov[4], M. Marta[4], M. Mostazo[6], I. Mukha[4], T. Neff[4], C. Nociforo[4], H. J. Ong[2], S. Pietri[4], A. Prochazka[4], C. Scheidenberger[4], B. Sitar[7], Y. Suzuki[8,9], M. Takechi[4], J. Tanaka[2], J. Vargas[6], J. S. Winfield[4], and H. Weick[4]

[1]*School of Physics and Nuclear Energy Engineering and IRCNPC, Beihang University, Beijing 100191, China*
[2]*RCNP, Osaka University, Ibaraki 567-0047, Japan*
[3]*Saint Mary's University, Halifax, NS B3H 3C3, Canada*
[4]*GSI Helmholtz Center, 64291 Darmstadt, Germany*
[5]*Department of Physics, Hokkaido University, Sapporo 060-0810, Japan*
[6]*Universidad de Santiago de Compostela, Santiago de Compostela 15782, Spain*
[7]*Comenius University, 818 06 Bratislava 16, Slovakia*
[8]*Department of Physics, Niigata University, Niigata 950-2181, Japan*
[9]*RIKEN Nishina Center, Wako 351-0198, Japan*
[*]E-mail: tanihata@rcnp.osaka-u.ac.jp, tera@buaa.edu.cn

Received July 12, 2014; Revised August 22, 2014; Accepted September 2, 2014; Published October 6, 2014

The charge-changing cross sections of $^{7,9-12,14}$Be have been measured at 900A MeV on a carbon target. These cross sections are discussed both in terms of a geometrical and a Glauber model. From several different analyses of the cross sections, the proton distribution radius (proton radius) of ^{14}Be is determined for the first time to be 2.41 ± 0.04 fm. A large difference in the proton and neutron radii is found. The proton radii are compared to the results of fermionic molecular dynamics (FMD) and antisymmetrized molecular dynamics (AMD) calculations.

Subject Index D12, D13

The nucleon distribution radii of unstable nuclei can be determined by several methods such as interaction cross sections [1,2] (σ_{I}) or reaction cross sections (σ_{R}) with light targets [2–4], and proton elastic scattering [5,6]. They have revealed new phenomena such as neutron halos and neutron skins [7] in neutron-rich nuclei.

Point proton distribution radii (called simply "proton radii" in what follows) of short-lived nuclei provide information about the structure of the nuclei complementary to the nucleon distribution radii. The proton radius is essential when a neutron halo is discussed. In addition, differences between the proton and neutron radii (the so-called "nuclear skin") help to determine the equation of state (EOS) at low temperatures, important for the study of neutron stars and stellar explosions. The proton radii of neutron-rich nuclei have previously been determined from the rms charge radii of the nuclei

determined by isotope-shift measurements [8]. However, the charge radius of ^{14}Be, which has a two-neutron halo [9–11], had not yet been measured. A measurement of proton radius would provide a means to study the correlation of two halo neutrons in ^{14}Be as was done in ^{6}He [12].

Determinations of the charge radii of light nuclei are extremely difficult for several reasons. First, it is difficult to produce cold ions or atoms of short-lived nuclei. Second, the isotope shifts are dominated by the mass shifts, which are not related to the radii. The field shift related to the radius can only be obtained by subtracting the theoretical mass shift from the observed value. Fortunately, owing to recent developments in ISOL techniques [12–16] and in atomic theory [17,18], the charge radii of He, Li, and Be were determined, except for ^{14}Be.

Consequently, it is desirable to have other methods to determine proton radii even if they are not as precise as isotope-shift measurements. Nucleon radii can be determined reasonably precisely using geometrical or Glauber models from $\sigma_{\rm I}$ measurements [2,19]. The charge-changing cross sections $\sigma_{\rm cc}$, when they are dominated by geometrical conditions similar to $\sigma_{\rm I}$, carry information about the proton distribution and proton radii [20]. Recently, the proton radii of $^{9-10}$Be, $^{14-16}$C, and $^{16-18}$O isotopes have been determined by Yamaguchi et al. from $\sigma_{\rm cc}$ using an empirical scaling law [21]. In the present experiment, the $\sigma_{\rm cc}$ of Be isotopes have been measured at about 900A MeV. Here the proton radius of ^{14}Be has been deduced by employing a geometrical analysis and from a Glauber analysis.

The relation between $\sigma_{\rm I}$ and nuclear size was first investigated using He-isotope experimental data [22]. The $\sigma_{\rm I}$ is written in terms of interaction radii determined empirically as

$$\sigma_{\rm I}(P,T) = \pi\left[R_{\rm I}(P) + R_{\rm I}(T)\right]^2, \tag{1}$$

where $R_{\rm I}(A)$ is the interaction radius of nucleus A, with P and T indicating the projectile and target nuclei, respectively. The predicted separation of the projectile and target radii in $\sigma_{\rm I}$ was experimentally tested by various projectiles and targets [1]. Supported by this geometrical result, a Glauber model for $\sigma_{\rm I}$ and $\sigma_{\rm R}$ has been developed and used to determine the rms radii of unstable nuclei [2,7,23].

Ignoring the effect of neutrons in a projectile, $\sigma_{\rm cc}$ in the optical limit can be written as

$$\sigma_{\rm cc} = \iint \left[1 - T_c(\mathbf{b})\right] d\mathbf{b}, \quad T_c(\mathbf{b}) = \left|\exp\left[i\chi(\mathbf{b})\right]\right|^2 \tag{2}$$

where $T_c(\mathbf{b})$ is the transmission function for proton removal from the projectile at impact parameter $\mathbf{b}$. The transmission function $T_c(\mathbf{b})$ is written by the phase shift function $\chi(\mathbf{b})$,

$$i\chi(\mathbf{b}) = \iint_P \iint_T \sum_i \left[\rho^z_{Pp}(\mathbf{s})\rho^z_{Ti}(\mathbf{t})\Gamma_{pi}(\mathbf{b}+\mathbf{s}-\mathbf{t})\right] d\mathbf{s}d\mathbf{t}, \tag{3}$$

with the thickness function ρ^z related to the density by, e.g.,

$$\rho^z_{Pi}(\mathbf{s}) = \int \rho_{Pi}\left(\sqrt{\mathbf{s}^2 + z^2}\right) dz, \tag{4}$$

where subscript $i = p$ or n indicates protons or neutrons, respectively, and z is the coordinate along the direction of the incident beam. The profile function

$$\Gamma_{ik}(\mathbf{b}) = \frac{1 - i\alpha_{ik}}{4\pi\beta^2_{ik}}\sigma_{ik}\exp\left(-\frac{\mathbf{b}^2}{2\beta^2_{ik}}\right) \tag{5}$$

describes the scattering of proton or neutron i, k with the appropriate parameter set [24]. The parameter β_{ik} in the profile function is the range of the nucleon–nucleon interaction and depends on the

Table 1. Charge-changing cross sections of Be+^{12}C [mb].

Nucleus	E/A [MeV]	C target	σ_I[mb]*[1]
^{7}Be	772	706 ± 8*[2]	739 ± 9
^{9}Be	921	682 ± 30	806 ± 9
^{10}Be	946	670 ± 10	813 ± 10
^{11}Be	962	681 ± 3	942 ± 8
^{12}Be	925	686 ± 3	927 ± 18
^{14}Be	833	697 ± 4	1089 ± 40
^{12}C	943	734 ± 6*[3]	853 ± 6
^{12}C FMA		727	854
^{12}C HO		724	852

*[1]Interaction cross sections (σ_I) from Refs. [1,9,27]. The energies of the incident beams are at around 800A MeV. The σ_I value shown for ^{14}Be is the average value of the values from Refs. [9,27]. Reference [2] tabulates all available cross section data.
*[2]The cross section is not corrected for the proton emission after neutron removal.
*[3]The present value is slightly larger than the value in Ref. [2] but is consistent within 2 standard deviations.

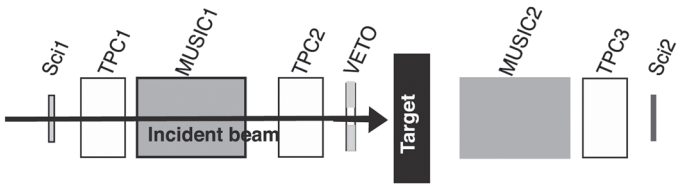

Fig. 1. The experimental setup. Sci: plastic scintillation detector, TPC: time-projection chamber, MUSIC: multi-sampling ion chamber.

beam energy. The parameter α_{ik}, the imaginary part of the profile function, does not affect the charge-changing cross section.

An energy-dependent scaling factor F is empirically introduced [21] based on the work of Bhagwat and Gambhir [25]:

$$\sigma_{\rm cc} = \int [1 - T_c(\mathbf{b})]\, F(E) d\mathbf{b}. \tag{6}$$

They found that the observed $\sigma_{\rm cc}$ are systematically larger than the calculated cross sections, and $F(E)$ is a smooth scaling function of the beam energy. It is equal to approximately 1.1 at 600A MeV and is probably smaller at higher energies. The present data also show enhanced cross sections, but only by a factor of 1.02–1.07 as shown later.

The $\sigma_{\rm cc}$ of Be isotopes were measured at the FRS facility of GSI in Germany. Incident beams of 1A GeV ^{40}Ar and ^{22}Ne were used to produce secondary beams of Be isotopes. The production target was 5 g/cm^2 thick Be. A carbon reaction target of thickness $t = 4.010$ g/cm^2 was used. The energies of the Be isotopes at the center of the target are listed in Table 1.

The experiments were performed at the final achromatic focus of FRS [26]. A block diagram of the detector system is presented in Fig. 1. Incident particles are identified by ΔE signals from MUSIC1 and the times of flight, which are determined by the time difference between the signals at the first plastic scintillator (Sci1) and at the other plastic scintillator placed at S2, the dispersive focus of the FRS located 36 m upstream.

The σ_{cc} are determined by the transmission method. The cross section is calculated by the ratio $\gamma = N_o/N_i$ of the numbers of incoming and outgoing nuclei with same Z as $\sigma_{cc} = (1/t)\ln(\gamma_{out}/\gamma_{in})$, where γ_{out} is the ratio without the target and γ_{in} is the ratio with the target in place. The incident beam identification is of high quality and fractional admixing of other nuclides is less than 10^{-4}. The Z of the nucleus after the target is identified by MUSIC2, where the ΔE signals are measured using eight anodes. Reactions in the MUSIC2 detector are infrequent and can be removed without influencing the final cross section because the effect is the same for target-in and target-out runs. For the present target thickness, $\gamma_{in} \approx 0.7$ and $\gamma_{out} \approx 0.96$.

Only the cross section for direct removal of protons is sought to determine proton radii. Therefore, reactions that only remove neutrons should not be counted as charge changing. However, such reactions appear as charge changing when ^{8}Be is produced by neutron removal from Be isotopes, because that nucleus decays immediately into a pair of ^{4}He nuclei. Since the decay energy is only 92 keV, the pair is emitted in almost the same direction in the laboratory with almost the same energy. They then give an energy signal corresponding to $Z = 2.83$, close to that of Li. A similar effect occurs for ^{6}Be during neutron removal from ^{7}Be. All proton dripline nuclei are subject to this problem because neutron removal results in proton emission. The decay energy of ^{6}Be is 1.4 MeV with a final state of $p + p + {}^4$He so that it is not possible to identify it using the present setup.

The pulse-height spectra of MUSIC2 in the $Z = 3$ region was investigated carefully in order to estimate the ^{8}Be effect. The observed pulse-height spectrum for a single charge was a good Gaussian shape down to 10^{-3} of the peak. The charge resolution of MUSIC2 was about $\Delta Z \sim 0.12$ in sigma. In the case of the ^{9}Be beam, the pulse-height distribution showed a wide peak at $Z \sim 2.8$ and a large shoulder at $Z \sim 3$. After subtraction of the $Z = 3$ peak assuming a Gaussian shape, a significant peak was observed at $Z = 2.75$ on top of the tail of the $Z = 2$ spectrum. The production of ^{8}Be was estimated from the counts in this peak, and the cross section was subtracted from the observed σ_{cc}. Although there was clear evidence of production of ^{8}Be by one-neutron removal, the determination of the associated cross section had a large uncertainty. For example, the peak position is not exactly at $Z = 2.83$, probably due to over-subtraction. In addition, the width of the two-^{4}He spectrum appears narrower than expected. For the case of ^{10}Be, the effect of two-^{4}He appears as a shoulder on the lower side of the $Z = 3$ peak, indicating a small contribution from ^{8}Be (two-neutron removal). No visible evidence of ^{8}Be was observed for the other neutron-rich isotopes of Be. The details of the analysis will be published elsewhere. The final results of the charge-changing cross sections are listed in Table 1. The results are also presented in Fig. 2. The experimental data are plotted as filled squares. The errors for ^{9}Be and ^{10}Be are larger than those for the other nuclei because of the additional uncertainties in the correction for ^{8}Be production as described above.

Firstly the σ_{cc} are calculated using the ^{12}C density distribution, which gives a charge radius consistent with $^{12}C + {}^{12}$C experiments. Both the fermionic molecular dynamics (FMD) and harmonic oscillator model densities are consistent with the observed value. A calculation for the σ_I also shows good agreement. Those values are shown in the last two columns of Table 1. The Glauber calculations are therefore valid for $^{12}C + {}^{12}$C cross sections. For Be isotopes, two different model density distributions are used: the FMD model combined with the unitary correlation operator method [27] and the antisymmetrized molecular dynamics (AMD) model [20].

The charge radii by the FMD model [30] reflect the structure of the isotopes, including the distance between alpha clusters and the formation of neutron halos. Strong mixings of sd configurations are important for ^{12}Be and ^{14}Be. These features are consistent with experimental results from one-neutron breakup reactions and interaction cross section measurements [11,31–33]. Although the

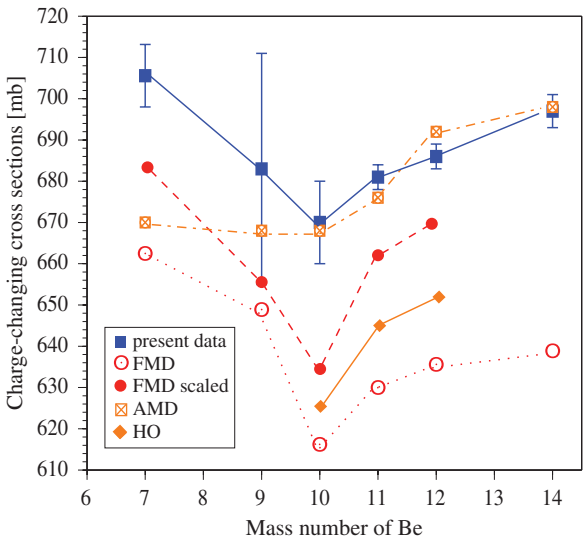

Fig. 2. Experimental and theoretical values of the σ_{cc}. 'FMD scaled' are the values corrected for the difference of experimental charge radii and FMD charge radii (see text).

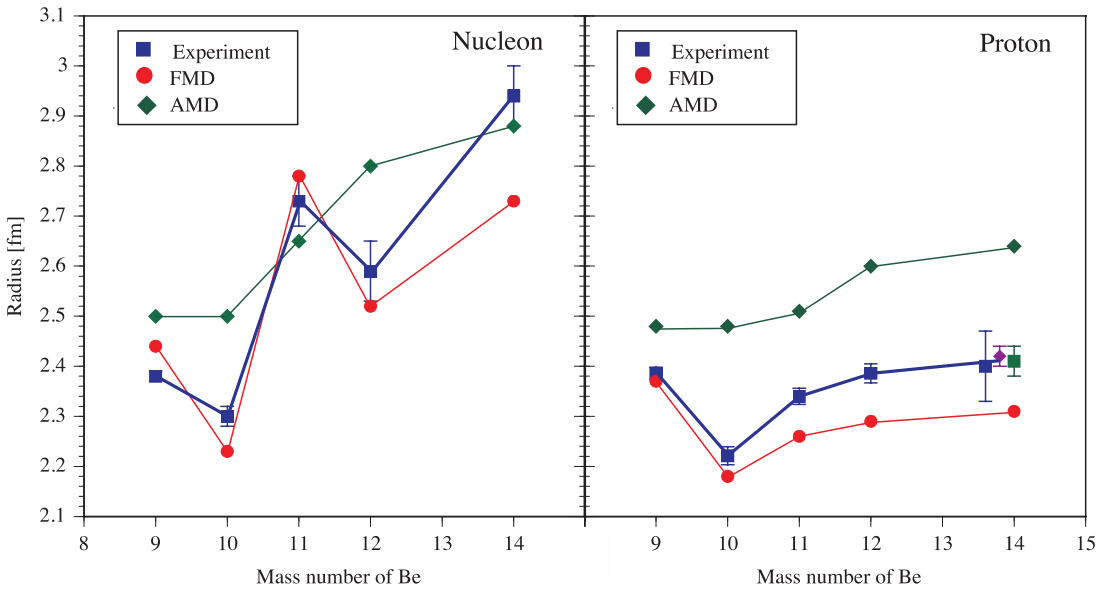

Fig. 3. Proton and nucleon rms radii of Be isotopes. Three values of the ^{14}Be proton radii determined by different methods described in the text are shown at mass numbers near 14 in the figure. The radii predicted by FMD and AMD calculations are also shown.

general trend in the radii for different isotopes is properly reproduced, the charge radii are smaller than the experimental values obtained from isotope-shift measurements [34,35].

The σ_{cc} of the Be isotopes are underestimated by about 7% in FMD, as shown in Fig. 2 by open circles. However, the proton radii of the FMD model are smaller than the observed value, as shown in Fig. 3. The cross sections scaled to account for these differences in radii are plotted in Fig. 2 by filled circles. The agreement is better, with discrepancies of less than 3%. The observed trend is correctly reflected. The matter radii of the FMD densities reproduce the observed matter radii to within a few percent, except for ^{14}Be where the deviation is 10%, as also shown in Fig. 3.

The AMD model calculations have previously been performed [28] using the Gogny D1S interaction and the same procedure is employed in the present calculations to obtain the density distributions. The basis wave functions for multi-configuration mixing are obtained using the matter quadrupole deformation as the generator coordinate. The AMD densities can account for the σ_{cc} as shown in Fig. 2. However, as seen in Fig. 3, the proton radii of the AMD densities are significantly larger than the experimental values. Furthermore, the matter distributions are reproduced for neither ^{10}Be nor ^{12}Be.

The diamonds in Fig. 2 show the Glauber results for harmonic oscillator density distributions of $^{10-12}$Be that reproduce the measured proton radii. They show the same behavior, as do the scaled FMD calculations, with only about 5% differences from the experimental values. As seen above, the Glauber model gives reasonable results if the correct proton radius is used. Recently, Horiuchi et al. have also tested such behavior [36].

The present model only uses the proton density distribution for the projectile nucleus and not the neutron distribution. The neutron density may affect the proton removal, and thus it should be taken into account in future work. The present geometrical model of the charge-changing cross sections is, however, valid to within a few percent. In particular, the relative changes in the proton radii are well described by the Glauber model. The geometrical interaction radius and the Glauber model are combined to evaluate the proton radius of ^{14}Be in the following discussion.

In the geometrical interaction radii model the σ_{cc} is modeled as $\sigma_{cc} = \pi[R_I(T) + R_{Ip}(P)]^2$, where $R_I = 2.61 \pm 0.02$ fm is the interaction radius of ^{12}C determined from the ^{12}C + ^{12}C reaction in Eq. (1). The interaction proton radius is R_{Ip}. Assuming that the rms proton radius R_p and the R_{Ip} are proportional to each other, the ratio $\Gamma = R_p/R_{Ip}$ can be used as a scaling factor. The average value of the ratio for ^{9}Be, ^{10}Be, ^{11}Be, and ^{12}Be is $\Gamma_{av} = 1.142 \pm 0.026$, which exhibits only a 2% fluctuation in the standard deviation. Next, R_p for ^{14}Be is determined from the measured value of σ_{cc} to be $\Gamma_{av} R_{Ip}(^{14}\text{Be}) = 2.40 \pm 0.07$ fm. Because ^{9}Be and ^{10}Be have extra uncertainties due to the ^{8}Be correction, the errors are much larger and result in a large fluctuation in Γ_{av}. Therefore these two isotopes were excluded from the average, giving $\Gamma_{av} = 1.147 \pm 0.014$. The value is not very different but the fluctuation is smaller. The deduced proton radius of ^{14}Be in this case is 2.42 ± 0.02 fm.

As already discussed, the Glauber results scale with the observed σ_{cc} if the known proton radii are used. Therefore, the Glauber model described by Eq. (2) is used here with a harmonic oscillator density [2]. The oscillator densities with two size parameters for protons and neutrons, a_p and a_n, are used. The size of ^{12}C is determined by the interaction cross section of ^{12}C + ^{12}C assuming that $a_p = a_n$. The σ_{cc} for ^{12}C + ^{12}C is well reproduced without using any scaling factor. Using the proton density distributions that reproduce the charge radii of $^{10-12}$Be, σ_{cc} are calculated by the Glauber model. The scaling factor F for the ratio of the experimental values to the calculated cross sections is found to be 1.071 ± 0.019. The difference between the Glauber model and the experimental values is only 7%. Using this factor, the size parameter of ^{14}Be is determined. The rms proton radius of ^{14}Be is then calculated to be 2.41 ± 0.03 fm. This value is also plotted in Fig. 3 as a diamond.

The experimentally determined proton and matter radii and those of the two theoretical models are also compared in Fig. 3. The AMD calculations [29] show larger radii for most of the isotopes. The FMD model underestimates the proton radii but the general trend from one isotope to another is roughly reproduced. The trend for the matter radii is also reasonably well predicted by the FMD calculations.

In summary, the charge-changing cross sections (σ_{cc}) of $^{7,9-12,14}$Be isotopes have been measured. The relation to the proton radii of the isotopes was studied using the geometrical and Glauber models.

A Glauber model of the σ_{cc} using FMD densities was found to underestimate the values by a few percent even after correcting it using the known charge radii of the Be isotopes. Nevertheless, the calculated σ_{cc} are proportional to the charge or proton radii. For this reason, a geometrical treatment of the σ_{cc} is a reasonable assumption. The proton radius of ^{14}Be was deduced using both the geometrical interaction radii model and the Glauber model. They gave consistent results with an overall value for the proton radius of $R_p = 2.41 \pm 0.06$ fm.

Acknowledgements

The support of the PR China government and Beihang University under the Thousand Talent program is gratefully acknowledged. The experiment is partly supported by the grant-in-aid program of the Japanese government under the contract number 23224008. This project is supported by NSERC, Canada. One of the authors (R.K.) gratefully acknowledges the HIC-4-FAIR program and JLU-Giessen for supporting part of this research stay.

References

[1] I. Tanihata et al., Phys. Rev. Lett. **55**, 2676 (1985).
[2] A. Ozawa, T. Suzuki, and I. Tanihata, Nucl. Phys. A **693**, 32 (2001).
[3] W. Mittig et al., Phys. Rev. Lett. **59**, 1889 (1987).
[4] M. Fukuda et al., Phys. Lett. B **268**, 339 (1991).
[5] P. Egelhof et al., Eur. Phys. J. A **15**, 27 (2002).
[6] A. V. Dobrovolsky et al., Nucl. Phys. A **766**, 1 (2006).
[7] I. Tanihata, H. Savajols, and R. Kanungo, Prog. Part. Nucl. Phys. **68**, 215 (2013).
[8] G. Huber et al., Phys. Rev. Lett. **34**, 1209 (1975).
[9] I. Tanihata et al., Phys. Lett. B **206**, 592 (1988).
[10] M. Zhar et al., Phys. Rev. C **48**, R1484 (1993).
[11] M. Labiche et al., Phys. Rev. Lett. **86**, 600 (2001).
[12] L.-B. Wang et al., Phys. Rev. Lett. **93**, 142501 (2004).
[13] P. Mueller et al., Phys. Rev. Lett. **99**, 252501 (2007).
[14] R. Sanchez et al., Phys. Rev. Lett. **96**, 033002 (2006).
[15] W. Nörtershäuser et al., Phys. Rev. Lett. **102**, 062503 (2009).
[16] A. Krieger et al., Phys. Rev. Lett. **108**, 142501 (2012).
[17] G. W. F. Drake, Nucl. Phys. A **737**, 25 (2004).
[18] Z.-C. Yan, W. Nörtershäuser, and G. W. Brake, Phys. Rev. Lett. **100**, 243002 (2008).
[19] M. Takechi et al., Phys. Rev. C **79**, 061601 (2009).
[20] I. Tanihata, Nucl. Instrum. Meth. A **532**, 79 (2004).
[21] T. Yamaguchi et al., Phys. Rev. Lett. **107**, 032502 (2011).
[22] I. Tanihata et al., Phys. Lett. B **160**, 380 (1985).
[23] Y. Ogawa, K. Yabana, and Y. Suzuki, Nucl. Phys. A **543**, 722 (1992).
[24] B. Abu-Ibrahim, W. Horiuchi, A. Kohama, and Y. Suzuki, Phys. Rev. C **77**, 034607 (2008).
[25] A. Bhagwat and Y. K. Gambihir, Phys. Rev. C **69**, 014315 (2004).
[26] H. Geissel et al., Nucl. Instrum. Meth. B **70**, 286 (1992).
[27] T. Suzuki et al., Nucl. Phys. A **658**, 313 (1999).
[28] T. Neff and H. Feldmeier, Eur. Phys. J. ST **156**, 69 (2008).
[29] Y. Kanada-Eny'o, M. Kimura, and H. Horiuchi, C.R. Phys. **4**, 497 (2003).
[30] A. Krieger et al., Phys. Rev. Lett. **108**, 142501 (2012).
[31] A. Navin et al., Phys. Rev. Lett. **85**, 266 (2000).
[32] S. D. Pain et al., Phys. Rev. Lett. **96**, 032502 (2006).
[33] T. Moriguchi et al., Nucl. Phys. A **929**, 83 (2006).
[34] R. Roth, T. Neff, and H. Feldmeier, Prog. Part. Nucl. Phys. **65**, 50 (2010).
[35] M. Kimura, Phys. Rev. C **69**, 044319 (2004).
[36] W. Horiuchi, Y. Suzuki, and T. Inakura, Phys. Rev. C **89**, 011601(R) (2014).